Golgi-modifying properties of macfarlandin E and the synthesis and evaluation of its 2,7-dioxabicyclo[3.2.1]octan-3-one core

Martin J. Schnermann[a], Christopher M. Beaudry[a], Anastasia V. Egorova[b], Roman S. Polishchuk[b,c], Christine Sütterlin[d,1], and Larry E. Overman[a,1]

[a]Department of Chemistry, 1102 Natural Sciences II, University of California, Irvine, CA 92697-2025; [b]Telethon Institute of Genetics and Medicine, Via P. Castellino 111, Naples, 8013, Italy; [c]Telethon Electron Microscopy Core Facility, Consorzio "Mario Negri Sud," Santa Maria Imbaro (CH), 66030, Italy; and [d]Department of Developmental and Cell Biology, 2011 Biological Sciences III, University of California, Irvine, CA 92697-2300

Contributed by Larry E. Overman, February 4, 2010 (sent for review January 18, 2010)

Golgi-modifying properties of the spongian diterpene macfarlandin E (MacE) and a synthetic analog, *t*-Bu-MacE, containing its 2,7-dioxabicyclo[3.2.1]octan-3-one moiety are reported. Natural product screening efforts identified MacE as inducing a novel morphological change in Golgi structure defined by ribbon fragmentation with maintenance of the resulting Golgi fragments in the pericentriolar region. *t*-Bu-MacE, which possesses the substituted 2,7-dioxabicyclo[3.2.1]octan-3-one but contains a *tert*-butyl group in place of the hydroazulene subunit of MacE, was prepared by chemical synthesis. Examination of the Golgi-modifying properties of MacE, *t*-Bu-MacE, and several related structures revealed that the entire oxygen-rich bridged-bicyclic fragment is required for induction of this unique Golgi organization phenotype. Further characterization of MacE-induced Golgi modification showed that protein secretion is inhibited, with no effect on the actin or microtubule cytoskeleton being observed. The conversion of *t*-Bu-MacE and a structurally related des-acetoxy congener to substituted pyrroles in the presence of primary amines in protic solvent at ambient temperatures suggests that covalent modification might be involved in the Golgi-altering activity of MacE.

organelle organization | chemical biology | natural product | reactivity

The use of small molecule natural products has been particularly fruitful in elucidating the dynamic features of Golgi organization and the role of this organelle in protein modification and transport. For example, brefeldin A (BFA, Fig. 1, **1**) induces loss of Golgi structure by enhancing retrograde transport of Golgi proteins to the endoplasmic reticulum (ER) (1). Studies with this natural product revealed key features of protein transport in the early secretory pathway and the role of the small GTPase, ADP-ribosylation factor (ARF) 1, in the regulation of membrane dynamics (2, 3). The diterpene ilimaquinone (IQ, Fig. 1, **2**) also induces reversible fragmentation of Golgi membranes into unisized vesicles (4), which might be the result of targeting components of the activated methyl cycle (5). Studies with IQ identified Gβγ and protein kinase D as previously undescribed regulators of Golgi structure and function (6–8). The activities of BFA and IQ contrast with those of the diterpene norrisolide (Fig. 1, **3**) and several synthetic analogs, which induce the irreversible conversion of Golgi stacks into dispersed fragments in the cytosol (9–12). Phospholipase A_2 (PLA_2) inhibitors also convert Golgi membranes into large punctate juxtanuclear structures indicating that PLA_2 may control the tubulation of the Golgi complex (13, 14). In addition, screens of natural product-inspired chemical libraries have identified compounds that block Golgi function in protein transport to the cell surface without affecting overall Golgi organization (15–17). Thus, identifying chemical entities that modify Golgi structure and function continues to offer fundamental insights into the function of this complex organelle.

The localization of the Golgi apparatus in close vicinity to the centrosome is typical for interphase mammalian cells. The specific localization of the Golgi is not required for general protein transport to the cell surface, but has recently been implicated in directional protein transport in a polarized cell (18–20). Screening of a library of small molecule marine natural products revealed that the marine metabolite, macfarlandin E (MacE, Fig. 2, **4**), impacts Golgi structure in a unique way: The Golgi ribbon is converted into small fragments that are maintained in the pericentriolar position of the cell. This phenotype contrasts with the effects of other small molecule natural products **1**, **2**, and **3** that cause Golgi fragmentation and concomitant loss of Golgi positioning. A detailed study of MacE would offer significant insight into the nature and mechanism of Golgi localization and organization; however, access to this natural product is limited to trace quantities (21). It was clear from the outset that further study would require a collaborative approach incorporating organic synthesis as a central element. We anticipated that a synthetic program would ultimately provide not only MacE, but also synthetic analogs whose evaluation would offer additional insights.

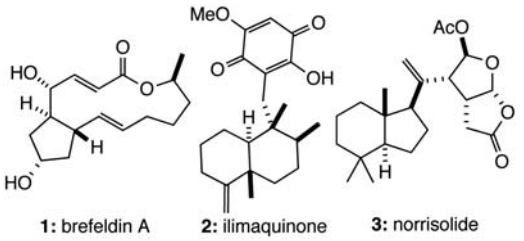

Fig. 1. Known Golgi-modifying agents.

Macfarlandin E, a member of a family of rearranged diterpenes, has been isolated from the dorid nudibranch *Chromodoris macfarlandi* and from two marine sponge species (21–23). Structurally, this diterpene is defined by a lipophilic *cis*-hydroazulene fragment joined to an oxygen-rich 2,7-dioxabicyclo [3.2.1]octan-3-one moiety. Despite its presence in 13 related natural products, including the closely related marine diterpene aplyviolene (**5**), no studies related to the synthesis of the 2, 7-dioxabicyclo[3.2.1]octan-3-one subunit had been disclosed

Author contributions: M.J.S., C.M.B., C.S., and L.E.O. designed research; M.J.S., C.M.B., A.V.E., R.S.P., and C.S. performed research; M.J.S., C.M.B., R.S.P., C.S., and L.E.O. analyzed data; M.J.S., C.S., and L.E.O. wrote the paper.

The authors declare no conflict of interest.

Data deposition: The atomic coordinates have been deposited in the Cambridge Structural Database, Cambridge Crystallographic Data Centre, Cambridge CB2 1EZ, United Kingdom [CSD reference nos. 762682 (**7**) and 762683 (**17**)].

[1]To whom correspondence may be addressed. E-mail: suetterc@uci.edu or leoverma@uci.edu

This article contains supporting information online at www.pnas.org/cgi/content/full/1001421107/DCSupplemental.

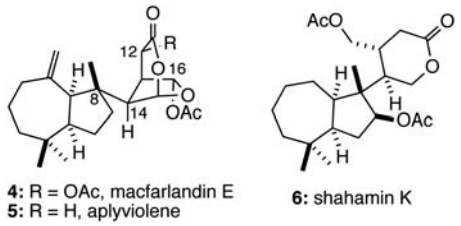

Fig. 2. Structures of macfarlandin E, aplyviolene, and shahamin K.

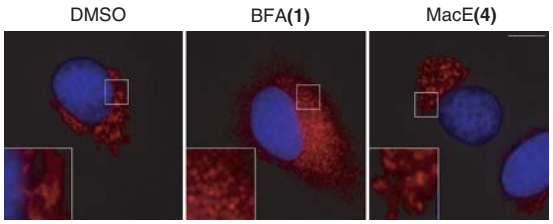

Fig. 3. MacE has a unique Golgi-modifying activity. NRK cells on coverslips were treated with DMSO, BFA (3 μg/mL), or MacE (20 μg/mL) for 60 min at 37 °C, fixed, and processed for immunofluorescence analysis with an antibody to the Golgi protein, giantin, and the DNA dye Hoechst 33342. The scale bar corresponds to 10 μM.

prior to this report (24). Shahamin K (**6**), which has an identical hydroazulene fragment, but a structurally simpler oxygenated fragment, was the initial rearranged spongian diterpene to be prepared by total synthesis (25).

Herein, we disclose the chemical synthesis of an analog of macfarlandin E (**4**), *t*-Bu-MacE (**7**, Scheme 1), that possesses the fully elaborated oxygenated subunit of the natural product, but has a lipophilic *tert*-butyl group in the place of the *cis*-hydroazulene subunit. We also describe the initial characterization of the Golgi-modifying properties of natural MacE, analog **7**, and several additional synthetic analogs, as well as the facile conjugation of analog **7** and its desacetoxy congener with primary amines to form pyrroles.

Results and Discussion

MacE Has a Unique Golgi-Modifying Activity. We identified MacE in a screen for compounds with Golgi-altering activity. MacE had a unique effect on Golgi organization as incubation of normal rat kidney (NRK) cells with this compound for 60 min at 37 °C induced the conversion of the continuous Golgi ribbon into small punctate structures in the pericentriolar region (Fig. 3 *Right*). This phenotype is fundamentally distinct from that observed with BFA (Fig. 3 *Middle*) and IQ, which caused Golgi relocalization into the ER or complete Golgi fragmentation and dispersal, respectively (1, 4). Additionally, MacE-induced Golgi fragments appeared much smaller than those produced by PLA_2 inhibitors (13). Thus, this phenotype appears to be unique in its nature. To complement this initial finding, we examined the effects of compounds obtained during the course of the total synthesis of shahamin K (**6**) (25), a collection that included both enantiomers of **6**, 14 compounds possessing the hydroazulene subunit, and the structurally closely related natural product aplyviolene (**5**).* The finding that none of these additional compounds were capable of inducing a Golgi fragmentation phenotype similar to that seen with MacE (**4**) suggests that the 2,7-dioxabicyclo[3.2.1]octan-3-one fragment is critical for the Golgi activity of this natural product.

Synthesis of Analogs Having the 2,7-Dioxabicyclo[3.2.1]octan-3-one Ring System. Guided by the absence of Golgi-modifying activity in structures possessing the hydroazulene motif, we selected as preliminary synthetic targets analogs **7** (*t*-Bu-MacE) and **8** that possess the intact oxygenated bridged-bicyclic subunit, yet incorporate a simple *tert*-butyl group in place of the hydroazulene moiety. Initial consideration of the structure of analogs **7** and **8** pointed to their potential genesis from a much simpler dialdehyde intermediate **9** (Scheme 1).† However, further analysis suggested that this concept likely would be unsuccessful in practice, because of unavoidable preferential formation of product **10** having the 2,8-dioxabicyclo[3.3.0]octan-3-one ring system found in norissolide (**3**) and many other structurally related natural products; this prediction follows from an expected kinetic preference for initial formation of a five-membered rather than a six-membered oxacyclic ring.

An alternative synthetic plan that addresses these concerns is outlined in retrosynthetic format in Scheme 1. It was envisaged that a late stage Baeyer–Villiger oxidation of the methyl ketone side chain of compound **11** would install the C16 acetoxy group (10, 26). This ketone was seen arising from acid-induced cyclization of acetal **12**, an intermediate in which oxocarbenium ion formation is limited to the C15 position. Lactol **12** can be simplified to acyclic precursor **13**, which we anticipated forming from enoxysilane **14** by oxidative cleavage of the cyclopentyl ring. Such a plan would establish the *cis* relationship between the *tert*-butyl and acetic acid side chains of intermediate **12** from a readily accessible 3,4-trans-disposed cyclopentenyl precursor **14**.

Guided by these considerations, we initiated the synthesis of analogs **7** and **8** by Mukaiyama–Michael reaction of enantiomerically enriched silyl ketene acetal **15** and cyclopentenone **16** (Scheme 2, 27–29). Subsequent elimination of acetic acid was induced by addition of water to the reaction mixture to produce enone **17**.‡ Reaction of **17** with aqueous trifluoroacetic acid removed the auxiliary, and the resulting acid was methylated to give cyclopentenone **18** (30). Coupling of this intermediate with *tert*-butylcyanocuprate in the presence of *tert*-butyldimethylsilyl chloride provided the transsubstituted cyclopentene **19** (31, 32). Takai olefination cleanly afforded an intermediate methyl enol ether, which underwent selective hydrolysis with oxalic acid to deliver methyl ketone **14** (33, 34). Oxidative cleavage of the double bond of **14** with osmium tetraoxide and sodium periodate, followed by reaction of the crude product with $TMSCHN_2$ provided tricarbonyl product **13** in high yield. After extensive screening, we discovered that reaction of **13** with camphorsulfonic acid and trimethyl orthoformate in methanol generated 2-methoxytetrahydrofuran dimethylacetal **20** as a 1:1 mixture of C15 epimers in acceptable yield.

With access to tetrahydrofuran intermediate **20**, we were able to readily construct the 2,7-dioxabicyclo[3.2.1]octan-3-one ring system (Scheme 3). Saponification of **20**, followed by ketal hydrolysis under acidic conditions, yielded carboxylic acid **12**. Cyclization of this intermediate with boron trifluoride etherate ($BF_3 \cdot OEt_2$) afforded 2,7-dioxabicyclo[3.2.1]octan-3-one **11**, which underwent Baeyer–Villiger oxidation with trifluoroperacetic acid to give analog **8** containing the dioxabicyclic fragment found in the rearranged spongian diterpene aplyviolene (**5**) (35).

After failing in numerous attempts to directly introduce an acetoxy substituent adjacent to the lactone carbonyl group of analog **8**, *t*-Bu-MacE (**7**) was prepared as summarized in the lower half of Scheme 3. Using the readily separable β-epimer of intermediate **20**, α-hydroxylation with oxaziridine **21** generated α-hydroxy ester **22** with high diastereoselectivity, albeit with the

*See *SI Appendix* for further information, including compounds that were screened and selected immunofluorescent results (*SI Appendix*).

†To simplify comparisons between synthetic analogs and MacE, the atom numbering of the natural product is used in *Results and Discussion*; proper atom numbering for synthetic molecules can be found in *SI Appendix*.

‡The relative configuration of this product was confirmed by single crystal x-ray diffraction analysis.

CHEMISTRY

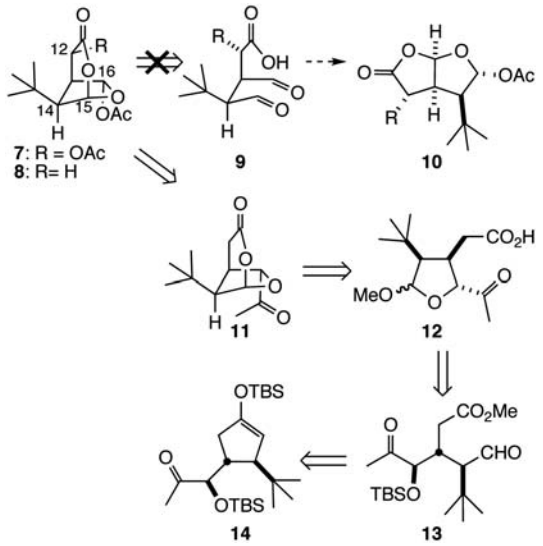

Scheme 1 Analysis of **7** and **8**.

opposite configuration at C12 of that found in MacE (36). The α-epimer of **20** was converted to the β-epimer by equilibration, allowing the overall efficiency of the conversion of **20** to **22** to be improved to 66% (two recycles).[§] Inverting the configuration at C16 was achieved in two steps by Dess–Martin oxidation to give the corresponding ketone, which was reduced with sodium borohydride in high diastereoselectivity (>20:1) to deliver **23** in 79% overall yield. Hydrolysis of the ester and the ketal, followed by acylation yielded α-acetoxy acid **24**, which, upon exposure to $BF_3 \cdot OEt_2$, converted to the bicyclic ketone **25** in high yield. Baeyer–Villiger oxidation of this product delivered *t*-Bu-MacE (**7**), whose structure was confirmed by single crystal x-ray analysis.

Effects of MacE and Its *t*-Butyl Analog on Golgi Organization and Function. Incubation of NRK cells with *t*-Bu-MacE (**7**) at 40 μg/mL produced a Golgi phenotype nearly identical to that of MacE (Fig. 4*A*). The Golgi ribbon was converted into small fragments that remained localized in the vicinity of the centrosome, as seen by immunofluorescence analysis of the cis-Golgi protein, giantin (Fig. 4*A*). Similar effects were also seen when we analyzed the organization of additional Golgi markers, including GRASP65 and β-COP (cis-Golgi), mannosidase II (medial Golgi), golgin-97 (trans-Golgi), or in HeLa cells (*SI Appendix*). These Golgi-modifying activities of MacE and *t*-Bu-MacE contrast to those of analogs **8**, **11**, and **25**, which had no effect on Golgi structure at concentrations of up to 80 μg/mL (*SI Appendix*). Intriguingly, *t*-Bu-MacE was less cytotoxic than MacE, as we observed extensive cell death when incubating cells with MacE (20 μg/mL) for 6 or 12 h, but not with *t*-Bu-MacE (40 μg/mL). This biological activity of MacE and its *tert*-butyl analog was specific for the Golgi apparatus, as the organization of the endoplasmic reticulum appeared unaltered (*SI Appendix*). In addition, the actin and microtubule cytoskeleton were normal after treatment of cells with these compounds for 60 min (*SI Appendix*).

On an ultrastructural level, MacE and *t*-Bu-MacE treatment induced significant alterations of Golgi morphology with disconnected and shorter Golgi stacks and extensively swollen cisternae being produced (Fig. 4*B* and *C*). In contrast, Golgi stacks in thin

[§]The high level of stereochemical control achieved in the hydroxylation reaction is readily rationalized by preferential orientation of the enolate away from the tetrahydrofuran ring and delivery of the oxygen electrophile to the face opposite the *tert*-butyl group.

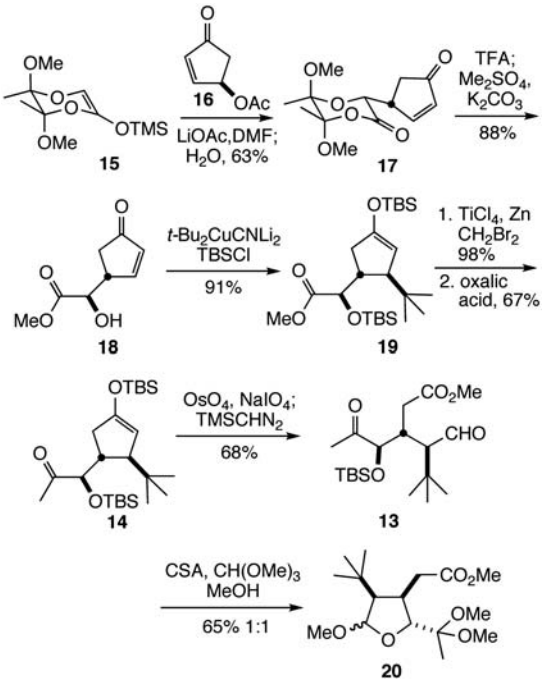

Scheme 2 Synthesis of **20**.

sections of DMSO-treated control cells contained usually five to six quite thin cisternae and were frequently connected into a ribbon-like structure.

The effect of MacE and *t*-Bu-MacE on the Golgi apparatus was irreversible. Fragmented Golgi membranes in the pericentriolar region were still seen after incubating MacE or *t*-Bu-MacE-treated cells in a fresh medium for 0.5 or 2 h (*SI Appendix*). Whereas incubating MacE or *t*-Bu-MacE-treated cells in a fresh medium for 5 h did not change the overall effect on Golgi

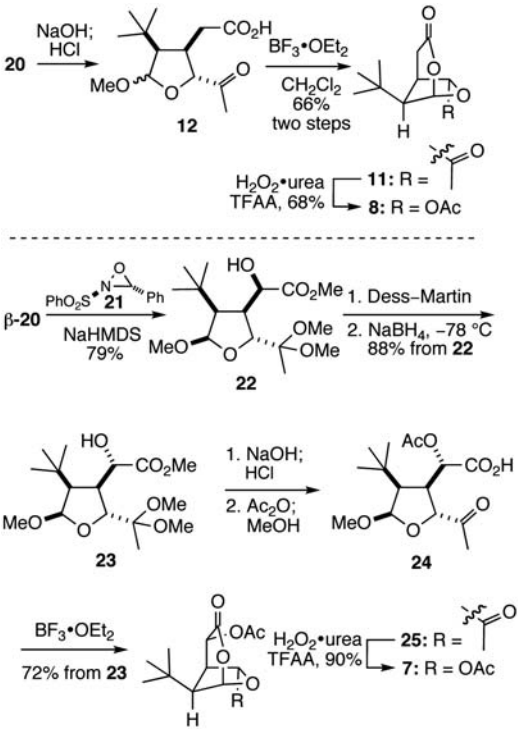

Scheme 3 Synthesis of **7** and **8**.

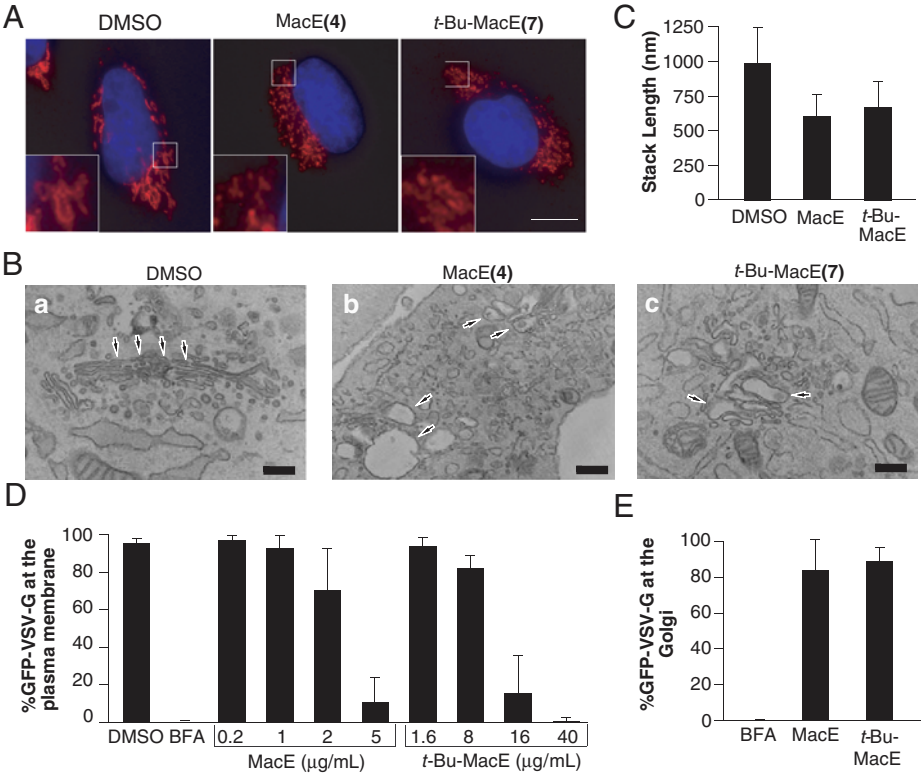

Fig. 4. Characterization of the Golgi-modifying activity of MacE and *t*-Bu-MacE (*A*) NRK cells on coverslips were treated with DMSO, MacE (20 μg/mL), *t*-Bu-MacE (40 μg/mL), fixed, and analyzed by immunofluorescence with an antibody to giantin. Magnifications of the boxed areas are shown in the insets. (*B*) NRK cells treated for 60 min with DMSO, 20 μg/mL MacE, or 40 μg/mL *t*-Bu-MacE were analyzed by electron microscopy. Arrows indicate the organization of Golgi membranes under these conditions. The scale bar for DMSO and *t*-Bu-MacE-treated cells corresponds to 300 nm, for MacE-treated cells to 510 nm. (*C*) Morphometric analysis was performed to determine the average length of Golgi stacks for each experimental condition. The values for MacE or *t*-Bu-MacE-treated cells are statistically distinct from the DMSO control (*t* test: $p < 0.01$). (*D*) Cells transfected with VSV-G^{tsO45}-GFP were incubated for 60 min with DMSO BFA (5 μg/mL) and indicated concentrations of MacE and *t*-Bu-MacE prior to fixation or incubation for 60 min to 32 °C. The fraction of cells with VSV-G^{tsO45}-GFP at the plasma membrane was determined for >100 cells per data point (see Fig. S4 for representative images, $n = 4$). (*E*) For BFA (5 μg/mL), MacE (20 μg/mL), *t*-Bu-MacE (40 μg/mL), the fraction of cells in which VSV-G^{tsO45}-GFP had reached the Golgi was determined in >100 cells ($n = 4$).

organization, we observed significant cell death in the population of MacE-treated cells. The irreversibility of this phenotype contrasts with that of other well-studied Golgi disrupting agents, such as brefeldin A, and suggests that the putative biological target of MacE or *t*-Bu-MacE may be modified covalently.

Given that **4** and **7** induced a significant change to the organization of the Golgi apparatus, we investigated if there was a concomitant block in protein transport. We performed vesicular stomatitus virus G protein (VSV-G) transport assays in which we first accumulated a GFP-tagged temperature sensitive form of VSV-G (VSV-G^{tsO45}-GFP) in the ER by incubating cells at a non-permissive temperature of 40.5 °C to prevent proper folding of this protein (37). During the last hour of this incubation, we treated the cells with MacE or *t*-Bu-MacE to induce Golgi fragmentation or with DMSO as a control. Then, we either fixed cells or shifted them to the permissive temperature of 32 °C, allowing VSV-G^{tsO45}-GFP to fold and be transported first to the Golgi and then to the cell surface (*SI Appendix*). With both **4** and **7**, we observed a concentration-dependent block of protein transport to the cell surface so that at the highest concentration, VSV-G^{tsO45}-GFP was no longer detected at the plasma membrane (Fig. 4*D*). It is of interest that at these concentrations of MacE and *t*-Bu-MacE, VSV-G^{tsO45}-GFP was able to reach the Golgi in most cells, although a substantial portion of this protein remained in the ER. This result suggests that protein transport between the ER and the Golgi is affected to a lesser extent than transport between the Golgi and the plasma membrane (Fig. 4*E*). We also examined effects of MacE and *t*-Bu-MacE on retrograde protein transport from the Golgi to the ER by treating cells first with these compounds for 60 min, followed by treatment with BFA for 45 min. We found that Golgi enzymes were able to undergo BFA-induced relocalization to the ER in the presence of both MacE and *t*-Bu-MacE, although relocalization was less complete than in control cells (*SI Appendix*). Together, these findings suggest that the effect of MacE and *t*-Bu-MacE on protein secretion is predominantly a result of a block in Golgi to plasma membrane transport.

Conjugation of *t*-Bu-MacE (7) and Analog 8 with Primary Amines. The plausibility of the 6-acetoxy-2,7-dioxabicyclo[3.2.1]octan-3-one moiety readily reacting with nucleophiles led us to examine the reactivity of *t*-Bu-MacE (**7**) and des-acetoxy analog **8** with biologically relevant nucleophiles. NMR and mass spectroscopic observation of the reaction of perdeutero-benzylamine and **7** in THF-d_8 at room temperature identified pyrrole **26**[¶] as the principal product (Scheme 4, 38). Notably, no intermediate species could be observed prior to the formation of **26** and equimolar quantities of acetic acid and benzyl acetamide. The pyrrole product **27**, which presumably derives through the intermediacy of **26**, can be isolated in moderate yield by sequential addition of benzylamine and camphorsulfonic acid (CSA) to a methanolic solution of **7**. As would be expected from these results, exposure of **8** to benzylamine generates the pyrrole product **28** in high yield

[¶]Efforts to isolate **26** have been complicated by the formation of additional products upon concentration.

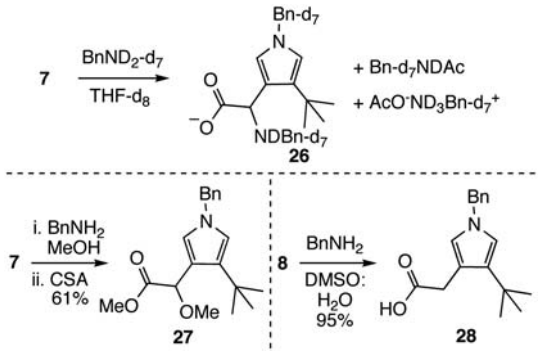

Scheme 4 In situ observation of **26** and synthesis of **27** and **28**.

(Scheme 4). A feasible mechanism to explain the conversion of the oxygenated core of *t*-Bu-MacE and analog **8** to pyrrole products consists of nucleophilic addition to the C16 acetoxy group and breakdown of the ensuing tetrahedral intermediate to generate a transient dialdehyde (**9**, Scheme 2) that subsequently undergoes Paal–Knorr-type pyrrole formation (39). Elimination of the C12 acetoxy group and benzylamine addition to the resultant α,β-unsaturated iminium leads to the formation of **26**. Subsequent addition of CSA promotes amine exchange with methanol and Fisher esterification to give **27**.

These findings highlight a potential functional role for the oxygenated dioxabicyclo[3.2.1]octanone as a masked 1,4-dialdehyde progenitor leading to a protein bound pyrrole species. The reaction of 1,4-dicarbonyl compounds with lysine residues to form pyrrole-protein conjugates has been proposed as the origin of cellular toxicity of *n* hexane via in vivo formation of 2,5-hexadione and levuglandin E_2, a δ-keto aldehyde derived from the prostaglandin precursor endoperoxide H_2 (40, 41). An additional feature, apparent from the observed formation of **26** and **27**, is the role of the C12 acetoxy group as a latent leaving group enabling the formation of structures that possess two sites of covalent modifications via pyrrole formation and subsequent C12 reactivity. The requirement of acetoxy groups at C12 and C16 to induce the unique Golgi phenotype reported herein suggests that pyrrole formation and potentially cross-linking might be involved in mediating the interaction of MacE and *t*-Bu-MacE with the putative biological target.

Conclusions. A unique Golgi phenotype has been identified for the spongian diterpene MacE (**4**) defined by fragmentation of the Golgi ribbon with localization of the Golgi fragments in the pericentriolar region and concurrent block of protein transport out of the Golgi. Limited access to significant quantities of the natural product prompted the development of a synthesis of the substituted dioxabicyclo[3.2.1]octanone ring system characteristic of MacE and related natural products. These studies included the synthesis of the truncated analog *t*-Bu-MacE, which induces the MacE Golgi phenotype, and other analogs whose biological studies outlined key elements of the structure activity relationships in this series. In addition, *t*-Bu-MacE was found to be less cytotoxic than MacE. The conversion of the oxygenated core of these MacE analogs to pyrrole products has suggested a potential mechanism of action for these compounds. Further studies directed at elucidating the target and the relevance of pyrrole-protein conjugate formation are under way. The synthetic methods described herein will serve to generate additional chemical structures that will facilitate these studies, as well as provide synthetic access to MacE.

Materials and Methods

Cell Culture. NRK and HeLa cells were grown in Advanced DMEM (Invitrogen), supplemented with 2% FBS and 2 mM glutaMAX-I (GIBCO) in a 5% CO_2 incubator.

Antibodies and Reagents Used in This Study. Anti-giantin, anti-β-COP and anti-GRASP65 (Sütterlin Lab), anti-Golgin-97 [kindly provided by Ed Chan (University of Florida)], anti-mannosidase II [kindly provided by Kelley Moreman (University of Georgia)], anti-calreticulin and anti-α-tubulin (Sigma) were used. BFA was from MP Biochemicals; phalloidin-Rhodamine was from Sigma. Fluorochrome-conjugated secondary antibodies were from Invitrogen.

Immunofluorescence. NRK or HeLa cells grown on coverslips were fixed for 10 min in 4% formaldehyde in PBS and incubated in blocking buffer (2.5% FBS, 0.1% Triton-X 100). Primary and secondary antibodies were diluted into blocking buffer. Cells were imaged with a Zeiss Axiovert 200M microscope and analyzed with linear adjustments with the Zeiss Axiovision software.

Compound Treatment. NRK cells on coverslips were treated with MacE, *t*-Bu-MacE, and BFA at the indicated concentration in complete medium supplemented with 25 mM Hepes pH 7.4 for the indicated periods of time. Control incubations were done with DMSO.

Electron Microscopy. NRK cells were grown in 6 well dishes and treated with DMSO, MacE, or *t*-Bu-MacE for 60 min. After their fixation with 1% glutaraldehyde in Hepes buffer, they were harvested by scraping, washed in PBS, embedded in Epon 812, and cut into thin sections. Analysis of thin sections was performed under a Tecnai-12 electron microscope (FEI/Philips). Images were taken using an ULTRA VIEW CCD digital camera. Morphometric analysis of Golgi stacks was performed in 20 cells (1–4 stacks per cell) for each experimental condition (overall; 41 stacks in DMSO, 38 in MacE, and 43 in *t*-Bu-MacE) using the ANALYSIS software.

Transport of VSV-G^{tsO45}-GFP. HeLa cells grown on coverslips were transfected with the plasmid VSV-G^{tsO45}-GFP (37) and left at 37 °C for 24 h. Cells were then shifted to 40.5 °C for 5 h and an additional 1 h in the presence of DMSO, MacE, or *t*-Bu-MacE. The cells were then fixed or shifted to 32 °C for 60 min to allow protein transport to the cell surface. Arrival of VSV-G^{tsO45}-GFP at the cell surface was quantified in at least 100 cells per each experimental condition.

Compounds. See *SI Appendix* for experimental details, ^1H and ^{13}C NMR spectra of previously undescribed compounds, and x-ray structures of *t*-Bu-MacE (**7**) and compound **17**.

ACKNOWLEDGMENTS. We thank Dr. Joe Ziller, University of California, Irvine, for the single-crystal x-ray analyses and Dr. John Greaves, University of California, Irvine, for mass spectrometric analyses. We gratefully acknowledge the late Professor John Faulkner, Scripps Institution of Oceanography (SIO), for encouragement and authentic macfarlandin E. We thank Professor Gerwick, SIO, and Dr. Hyukjae Choi, SIO, for purification and access to authentic aplyviolene. This research was supported by the NIH Neurological Disorders & Stroke Institute (Grant NS-12389) and by NIH postdoctoral fellowship support for M.J.S. (CA-138084) and C.M.B. (GM-079937). NMR, mass spectra, and the x-ray analyses were obtained at UC Irvine using instrumentation acquired with the assistance of NSF and NIH Shared Instrumentation grants. Unrestricted funds from Amgen, Merck, and Roche Biosciences are also gratefully acknowledged.

1. Klausner RD, Donaldson JG, Lippincott-Schwartz J (1992) Brefeldin A: Insights into the control of membrane traffic and organelle structure. *J Cell Biol* 116:1071–1080.
2. Donaldson JG, Finazzi D, Klausner RD (1992) Brefeldin A inhibits Golgi membrane-catalysed exchange of guanine nucleotide onto ARF protein. *Nature* 360:350–352.
3. Renault L, Guibert B, Cherfils J (2003) Structural snapshots of the mechanism and inhibition of a guanine nucleotide exchange factor. *Nature* 426:525–530.
4. Takizawa PA, et al. (1993) Complete vesiculation of Golgi membranes and inhibition of protein-transport by a novel sea sponge metabolite, ilimaquinone. *Cell* 73:1079–1090.
5. Radeke HS, Digits CA, Casaubon RL, Snapper ML (1999) Interactions of (–)-ilimaquinone with methylation enzymes: Implications for vesicular-mediated secretion. *Chem Biol* 6:639–647.
6. Jamora C, et al. (1997) Regulation of Golgi structure through heterotrimeric G proteins. *Cell* 91:617–626.
7. Jamora C, et al. (1999) Gβγ-Mediated regulation of Golgi organization is through the direct activation of protein kinase D. *Cell* 98:59–68.
8. Liljedahl M, et al. (2001) Protein kinase D regulates the fission of cell surface destined transport carriers from the trans-Golgi network. *Cell* 104:409–420.

9. Brady TP, et al. (2004) Fragmentation of Golgi membranes by norrisolide and designed analogues. *Bioorg Med Chem Lett* 14:5035–5039.
10. Brady TP, Kim SH, Wen K, Theodorakis EA (2004) Stereoselective total synthesis of (+)-norrisolide. *Angew Chem, Int Ed* 43:739–742.
11. Guizzunti G, Brady TP, Malhotra V, Theodorakis EA (2006) Chemical analysis of norrisolide-induced Golgi vesiculation. *J Am Chem Soc* 128:4190–4191.
12. Guizzunti G, Brady TP, Malhotra V, Theodorakis EA (2007) Trifunctional norrisolide probes for the study of Golgi vesiculation. *Bioorg Med Chem Lett* 17:320–325.
13. De Figueiredo P, Drecktrah D, Katzenellenbogen JA, Strang M, Brown WJ (1998) Evidence that phospholipase A2 activity is required for Golgi complex and trans Golgi network membrane tubulation. *Proc Natl Acad Sci USA* 95:8642–8647.
14. De Figueiredo P, Polizotto RS, Drecktrah D, Brown WJ (1999) Membrane tubule-mediated reassembly and maintenance of the Golgi complex is disrupted by phospholipase A2 antagonists. *Mol Biol Cell* 10(6):1763–1782.
15. Goess BC, Hannoush RN, Chan LK, Kirchhausen T, Shair MD (2006) Synthesis of a 10,000-membered library of molecules resembling carpanone and discovery of vesicular traffic inhibitors. *J Am Chem Soc* 128:5391–5403.
16. Pelish HE, Westwood NJ, Feng Y, Kirchhausen T, Shair MD (2001) Use of biomimetic diversity-oriented synthesis to discover galanthamine-like molecules with biological properties beyond those of the natural product. *J Am Chem Soc* 123:6740–6741.
17. Pelish HE, et al. (2006) Secramine inhibits Cdc42-dependent functions in cells and Cdc42 activation *in vitro*. *Nat Chem Biol* 2:39–46.
18. Preuss D, Mulholland J, Franzusoff A, Segev N, Botstein D (1992) Characterization of the Saccharomyces Golgi complex through the cell cycle by immunoelectron microscopy. *Mol Biol Cell* 3:789–803.
19. Cole NB, Sciaky N, Marotta A, Song J, Lippincott-Schwartz J (1996) Golgi dispersal during microtubule disruption: Regeneration of Golgi stacks at peripheral endoplasmic reticulum exit sites. *Mol Biol Cell* 7:631–650.
20. Yadav S, Puri S, Linstedt AD (2009) A primary role for Golgi positioning in directed secretion, cell polarity, and wound healing. *Mol Biol Cell* 20:1728–1736.
21. Molinski TF, Faulkner DJ, He CH, Van Duyne GD, Clardy J (1986) Three new rearranged spongian diterpenes from *Chromodoris macfarlandi*: Reappraisal of the structures of dendrillolides A and B. *J Org Chem* 51:4564–4567.
22. Hambley TW, Poiner A, Taylor WC (1986) Diterpene metabolites of the marine sponge *Chelonaplysilla violacea*: Aplyviolene and aplyviolacene. *Tetrahedron Lett* 27:3281–3282.
23. Carmely S, Cojocaru M, Loya Y, Kashman Y (1988) Ten new rearranged spongian diterpenes from two Dysidea species. *J Org Chem* 53:4801–4807.
24. Keyzers RA, Northcote PT, Davies-Coleman MT (2006) Spongian diterpenoids from marine sponges. *Nat Prod Rep* 23:321–334.
25. Lebsack AD, Overman LE, Valentekovich RJ (2001) Enantioselective total synthesis of shahamin K. *J Am Chem Soc* 123:4851–4852.
26. Krow GR (1993) The Baeyer–Villiger oxidation of ketones and aldehydes. *Org Reactions* 43:251–352.
27. Ley SV, Dixon DJ, Guy RT, Rodriguez F, Sheppard TD (2005) Michael, Michael–aldol and Michael–Michael reactions of enolate equivalents of butane-2,3-diacetal protected glycolic acid derivatives. *Org Biomol Chem* 3:4095–4107.
28. Nakagawa T, Fujisawa H, Nagata Y, Mukaiyama T (2004) Lithium acetate-catalyzed Michael reaction between trimethylsilyl enolate and α,β-unsaturated carbonyl compound. *Chem Lett* 33:1016–1017.
29. Hughes CC, Miller AK, Trauner D (2005) An electrochemical approach to the guanacastepenes. *Org Lett* 7:3425–3428.
30. Ley SV, et al. (1998) Total synthesis of the protein phosphatase inhibitor okadaic acid. *J Chem Soc Perkin Trans 1* 1:3907–3911.
31. Corey EJ, Kang M, Desai MC, Ghosh AK, Houpis IN (1988) Total synthesis of (+/–)-ginkgolide B. *J Am Chem Soc* 110:649–651.
32. Corey EJ, Boaz NW (1985) The reactions of combined organocuprate-chlorotrimethylsilane reagents with conjugated carbonyl compounds. *Tetrahedron Lett* 26:6019–6022.
33. Roberts SW, Rainier JD (2007) Synthesis of an A–E gambieric acid subunit with use of a C-glycoside centered strategy. *Org Lett* 9:2227–2230.
34. Takai K, et al. (1996) Alkylidenation of ester carbonyl groups: (Z)-1-ethoxy-phenyl-1-hexene. *Org Synth* 73:73–84.
35. Cooper MS, Heaney H, Newbold AJ, Sanderson WR (1990) Oxidation reactions using urea-hydrogen peroxide; a safe alternative to anhydrous hydrogen peroxide. *Synlett* 533–535.
36. Vishwakarma LC, Stringer OD, Davis FA (1988) (+/–)-*trans*-2-(phenylsulfonyl)-3-phenyloxaziridine. *Org Synth* 66:203–210.
37. Hirschberg K, et al. (1998) Kinetic analysis of secretory protein traffic and characterization of golgi to plasma membrane transport intermediates in living cells. *J Cell Biol* 143:1485–1503.
38. Laschat L, Grehl M (1994) Diastereoselective synthesis of α-hydroxy and α-aminoindolizidines and quinolizidines. Evidence for a novel cyclization/hydride migration mechanism in the $TiCl_4$-induced reaction of prolinal benzylamines by deuterium labeling studies. *Chem Ber* 127:2023–2034.
39. Gribble GW (2005) *Name Reactions in Heterocyclic Chemistry*, ed JJ Lie (Wiley, Hoboken, NJ), pp 79–88.
40. DeCaprio AP, Jackowski SJ, Regan KA (1987) Mechanism of formation and quantitation of imines, pyrroles, and stable nonpyrrole adducts in 2,5-hexanedione-treated protein. *Mol Pharmacol* 32:542–548.
41. Iyer RS, Kobierski ME, Salomon RG (1994) Generation of pyrroles in the reaction of levuglandin E(2) with proteins. *J Org Chem* 59:6038–6043.